JACS
JOURNAL OF THE AMERICAN CHEMICAL SOCIETY
Communication
pubs.acs.org/JACS

Giant Negative Thermal Expansion in $NaZn_{13}$-Type La(Fe, Si, Co)$_{13}$ Compounds

Rongjin Huang,[†,‡] Yanying Liu,[§] Wei Fan,[†] Jie Tan,[†] Furen Xiao,[§] Lihe Qian,[§] and Laifeng Li*[,†,‡]

[†]Key Laboratory of Cryogenics, Technical Institute of Physics and Chemistry, Chinese Academy of Sciences, Beijing, China
[‡]State Key Laboratory of Technologies in Space Cryogenic Propellants, Technical Institute of Physics and Chemistry, Chinese Academy of Sciences, Beijing, China
[§]State Key Laboratory of Metastable Materials Science and Technology, Yanshan University, Qinhuangdao, China

Supporting Information

ABSTRACT: La(Fe, Si)$_{13}$-based compounds are well-known magnetocaloric materials, which show a pronounced negative thermal expansion (NTE) around the Curie temperature but have not been considered as NTE materials for industrial applications. The $NaZn_{13}$-type $LaFe_{13-x}Si_x$ and $LaFe_{11.5-x}Co_xSi_{1.5}$ compounds were synthesized, and their linear NTE properties were investigated. By optimizing the chemical composition, the sharp volume change in La(Fe, Si)$_{13}$-based compounds was successfully modified into continuous expansion. By increasing the amount of Co dopant in $LaFe_{11.5-x}Co_xSi_{1.5}$, the NTE shifts toward a higher temperature region, and also the NTE operation-temperature window becomes broader. Typically, the linear NTE coefficient identified in the $LaFe_{10.5}Co_{1.0}Si_{1.5}$ compound reaches as much as -26.1×10^{-6} K^{-1}, with an operation-temperature window of 110 K from 240 to 350 K, which includes room temperature. Such control of the specific composition and the NTE properties of La(Fe, Si)$_{13}$-based compounds suggests their potential application as NTE materials.

It is well-known that the vast majority of materials have a positive coefficient of thermal expansion (CTE). Nevertheless, some other materials contract upon heating, and this phenomenon is called negative thermal expansion (NTE). Such NTE materials can be mixed with materials showing positive thermal expansion to form composites with precisely tailored CTE. Hence, there are a number of important potential applications of NTE materials used as, for example, optical fiber reflective grating devices, high-precision optical mirrors, printed circuit boards, and machinery parts.[1,2] Up to the present time several classes of materials have been identified and studied for their potential as NTE materials. In addition to the well-known ZrW_2O_8 family of materials, NTE behavior has also been reported in silicates such as β-$LiAlSiO_4$ (β-eucryptite), cyanides such as $Cd(CN)_2$, as well as ReO_3,[3,4] CuO nanoparticles,[5] ScF_3,[6,7] $PbTiO_3$-based compounds,[8] and antiperovskite manganese nitride.[9−12] However, only a very limited number of NTE materials serve as thermal expansion compensators in practice, due to the relatively narrow NTE operation-temperature window, low NTE coefficient, thermal expansion anisotropy, as well as low mechanical and/or electrical insulating properties.[13] To promote an even wider range of practical applications, it has long been desired to develop new materials with better NTE performances.

La(Fe, Si)$_{13}$-based compounds with $NaZn_{13}$-type structure (space group $Fm\bar{3}c$), first reported by Palstra et al. in 1983, demonstrate a variety of anomalous critical behavior due to their peculiar relationship between magnetism and crystal structure. As shown in the inset of Figure 1, the sites of La(8a), Fe$_I$(8b), and Fe$_{II}$(96i) are occupied by the atoms of La, Fe, and Fe(and/or Si), respectively. Recently, La(Fe, Si)$_{13}$-based compounds have attracted much attention because of their excellent magnetocaloric effect (MCE)[14−16] and potential applications in magnetic refrigeration. The MCE in this type of material is mainly attributed to the itinerant electron metamagnetic (IEM) transition, i.e., a field-induced first-order transition from the PM state to the FM state. However, if the relationship between magnetism and crystal structure under the condition of nonexternal magnetic field is considered, it is found that the crystal lattice undergoes a change accompanied by a magnetic phase transition, i.e., magnetovolume effect (MVE) occurs. For example, the lattice cell of the $LaFe_{11.4}Si_{1.6}$ compound shows a pronounced, large NTE around the Curie

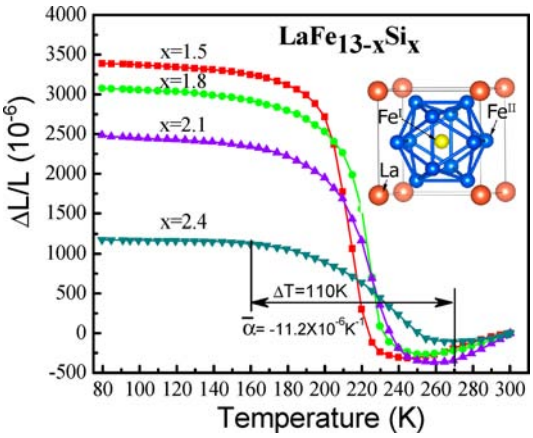

Figure 1. Temperature dependence of linear thermal expansions $\Delta L/L$ (reference temperature: 300 K) of $LaFe_{13-x}Si_x$ (x = 1.5, 1.8, 2.1, and 2.4) in the temperature range of 77−300 K. (Inset) Crystal structure.

Received: May 23, 2013
Published: July 25, 2013

 © 2013 American Chemical Society dx.doi.org/10.1021/ja405161z | J. Am. Chem. Soc. 2013, 135, 11469−11472

temperature, accompanied by a first-order phase transition.[14] Therefore, from a technological viewpoint, La(Fe, Si)$_{13}$-based compounds, with an excellent MCE, are also promising potential candidates as NTE materials.

Although much effort has been focused on the La(Fe, Si)$_{13}$-based magnetocaloric materials with a first order phase transition, attempting to obtain large isothermal magnetic entropy change (ΔS_M), however, these La(Fe, Si)$_{13}$-based compounds have not been considered as NTE materials for industrial applications. Motivated by the sudden and pronounced increase in volume with decreasing temperature, we tried to convert the first-order phase transition of La(Fe, Si)$_{13}$-based compounds to the second-order one and to achieve optimized design of materials with large NTE coefficients as well as broad NTE operation-temperature windows, covering room temperature. Indeed, by systematically investigating the NTE properties of $LaFe_{13-x}Si_x$ and $LaFe_{11.5-x}Co_xSi_{1.5}$ and optimizing the Si and Co contents, the sharp volume change was successfully modified into continuous expansion. A large NTE coefficient of -26.1×10^{-6} K^{-1} in the temperature range from 240 to 350 K, which includes room temperature, and a broad NTE operation-temperature window of 110 K were obtained in the $LaFe_{10.5}Co_{1.0}Si_{1.5}$ compound.

All measurements were carried out using polycrystalline samples. A series of $LaFe_{13-x}Si_x$ and $LaFe_{11.5-x}Co_xSi_{1.5}$ compounds were prepared in an arc melting furnace under a high-purity argon atmosphere. The raw materials of Fe, Co, Si, and La were at least 99.99% pure. An excess 10 at % of La over the stoichiometric composition was added to compensate for loss during melting. Button samples were melted four times, and each time during melting the buttons were turned over to ensure homogeneity. The arc-melted ingots wrapped by Ta foils were sealed in a quartz tube filled with high-purity argon gas, subsequently homogenized at 1050 °C for 30 days, and finally quenched quickly into cold water. In situ powder XRD was employed to identify the phase constitutions and crystal structure at different temperatures. The linear thermal expansion data ($\Delta L/L$) vs temperature curves were obtained by a thermo-dilatometer with a heating rate of 2 K/min. The electrical resistivity and thermal conductivity were measured using a standard four-probe method and a steady state method, respectively. The magnetization was measured as a function of temperature in an applied field of 0.3 T using a SQUID-VSM.

Figure 1 displays linear thermal expansion ($\Delta L/L$) data (reference temperature: 300 K) as a function of temperature for $LaFe_{13-x}Si_x$ (x = 1.5, 1.8, 2.1, and 2.4). It can be seen that for each sample there exists a temperature region in which the linear thermal expansion $\Delta L/L$ increases with decreasing temperature, i.e., NTE occurs. Moreover, the NTE properties are strongly affected by partial substitution of Si for Fe. The $LaFe_{11.5}Si_{1.5}$ exhibits a sharp volume change in a temperature range from 170 to 240 K, and the NTE operation-temperature window (ΔT) is 70 K. The variation of $\Delta L/L$ is estimated to be 3.5×10^{-3}, which is comparable to those of antiperovskite manganese nitrides Mn_3ZnN (4.6×10^{-3})[9] and Mn_3GaN (3.8×10^{-3}).[17] The temperature range for linear expansion gradually becomes broader with increasing the amount of Si from 1.5 to 2.4. The gradual linear expansion gives rise to a large negative slope over a wide temperature range. The NTE in the $LaFe_{11.2}Si_{1.8}$ occurs in the temperature range from 165 to 250 K (ΔT = 85 K), whereas the NTEs of the $LaFe_{10.9}Si_{2.1}$ and the $LaFe_{10.6}Si_{2.4}$ take place from 160 to 260 K (ΔT = 100 K) and from 160 to 270 K (ΔT = 110 K), respectively. This fact indicates that the partial substitution of Si for Fe plays an important role in broadening NTE operation-temperature window.

On the other hand, it should be noted that the variation of $\Delta L/L$ versus temperature in the NTE region decreases with increasing Si content, resulting in a decreased NTE coefficient. For example, the $LaFe_{11.5}Si_{1.5}$ shows an average CTE of -50.1×10^{-6} K^{-1} between 170 and 240K (ΔT = 70 K), but the average CTE for $LaFe_{10.6}Si_{2.4}$ is -11.2×10^{-6} K^{-1} between 160 and 270 K (ΔT = 110 K). Furthermore, another two interesting features are observed from Figure 1. The first one is that the variation of $\Delta L/L$ is small in the temperature range from 77 to 160 K. The second one is that the $\Delta L/L$ at liquid nitrogen temperature (77 K) is larger than that at room temperature, meaning that the average CTE is negative in the temperature range from liquid nitrogen temperature to room temperature. Specifically, the average CTEs of the $LaFe_{11.5}Si_{1.5}$ and the $LaFe_{10.6}Si_{2.4}$ are -15.2×10^{-6} K^{-1} and -5.4×10^{-6} K^{-1} in the temperature range from 77 to 300 K, respectively.

Although the $LaFe_{13-x}Si_x$ shows a giant NTE, the NTE operation-temperature window of all the samples appears at cryogenic temperatures. To promote wider applications, it is highly desirable that the NTE takes place near room temperature. Additionally, the absolute values of the NTE coefficient rapidly decrease with increasing Si content. This is unfavorable for obtaining material with large NTE coefficients. To further improve performance, we tried "doping", i.e., partial substitution of Co for Fe based on the $LaFe_{11.5}Si_{1.5}$. Figure 2a displays linear thermal expansion data (reference temperature:

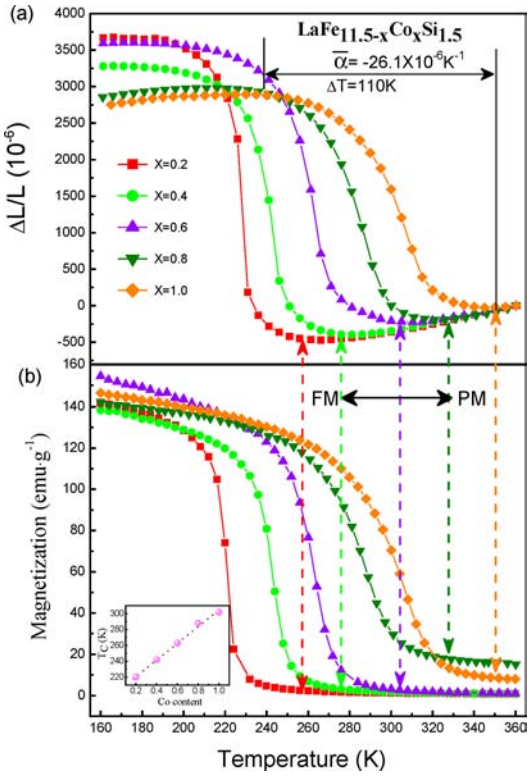

Figure 2. (a) Temperature dependence of linear thermal expansions $\Delta L/L$ (reference temperature: 360 K) and (b) temperature dependence of magnetizations for $LaFe_{11.5-x}Co_xSi_{1.5}$ (x = 0.2, 0.4, 0.6, 0.8, and 1.0). (Inset) Curie temperatures of $LaFe_{11.5-x}Co_xSi_{1.5}$ (x = 0.2, 0.4, 0.6, 0.8, and 1.0).

dx.doi.org/10.1021/ja405161z | J. Am. Chem. Soc. 2013, 135, 11469−11472

360 K) as a function of temperature for $LaFe_{11.5-x}Co_xSi_{1.5}$ (x = 0.2, 0.4, 0.6, 0.8, and 1.0). It can be seen that, similarly to increasing Si content, increasing Co content also plays an efficient role in broadening NTE operation-temperature window, and the volume change due to NTE becomes gradual with increasing Co content. Specifically, the NTE operation-temperature window of the $LaFe_{11.3}Co_{0.2}Si_{1.5}$ and the $LaFe_{11.1}Co_{0.4}Si_{1.5}$ are 74 and 90 K, respectively, whereas for $LaFe_{10.5}Co_{1.0}Si_{1.5}$, the NTE operation-temperature window reaches 110 K. Furthermore, by substituting Fe with a certain amount of Co, the NTE operation-temperature window moves toward a higher temperature region, and the change value of the $\Delta L/L$ within the NTE operation-temperature window decreases less rapidly with increasing Co content than that with increasing Si content. The NTE operation-temperature window of the $LaFe_{10.5}Co_{1.0}Si_{1.5}$ starts from 240 to 350 K (ΔT = 110 K), covering room temperature, and yields an average CTE of $\alpha = -26.1 \times 10^{-6}\ K^{-1}$, which is about 3 times larger than that of the commercial NTE materials currently used, i.e., ZrW_2O_8 with $\alpha = -9 \times 10^{-6}\ K^{-1}$. The absolute magnitude of this negative CTE is comparable to those of high-expansion metals such as Al ($23 \times 10^{-6}\ K^{-1}$ at room temperature).

As mentioned above, the crystal lattice parameter of La(Fe, $Si)_{13}$-based compounds undergoes a change due to the magnetovolume effect, which is associated with the increased of kinetic energy of the electron system. To break the magnetic order in FM state at low temperature, the itinerant electron system needs to absorb energy. When this amount of energy is larger than what originates from thermal fluctuation, the crystal lattice will contract to compensate for an extra need. Figure 2 shows that all samples undergo an FM to PM transition and the NTE behavior occurs around the magnetic transition temperature. The starting temperature of NTE is consistent with that of magnetic transition, which confirms the strong coupling of the thermal expansion behavior with the magnetic transition. Figure 3 shows the rates of change of the magnetization (dM/dT) as a function of temperature. The linear thermal expansion $\Delta L/L$ is affected by the dM/dT. In the green slash region, the dM/dT is negative and the absolute value of dM/dT is relatively large, and thus the NTE behavior appears. It suggests that the lattice expansion induced by the magnetic transition is larger than the thermal contraction due to the temperature decrease. It was reported that magnetic transition temperature is affected by the variation in the density of 3d electron at the Fermi level caused by the different 3d-elements substitution, which contributes different numbers of electrons to the conduction band.[18,19] When dopants with more moments are introduced, the energetic need to trigger phase transition will be higher. Therefore, a higher transition temperature is expected. It is observed from the inset of Figure 2 that the magnetic transition temperature (T_c) of $LaFe_{11.5-x}Co_xSi_{1.5}$ (x = 0.2, 0.4, 0.6, 0.8, and 1.0) increases with increasing Co contents, which is most likely due to the increase of 3d electron number caused by partially substituting Fe by Co. Accordingly, the NTE operation-temperature window moves toward the higher temperature region. On the other hand, it was reported that the Fe_I–Fe_{II} distance plays the critical role in the exchange interaction.[20] With increasing Co/Si content, the Fe_I–Fe_{II} distance increases due to the smaller atomic size of Co/Si compared to that of Fe,[20] which enhances the positive exchange interaction and may break the long-range magnetic order in Fe and help to form local magnetic domains. As a result, magnetic phase transition takes place gradually rather than a sharp change. Figure 2 shows that the width of the NTE operation-temperature window is also associated with magnetic transition. The magnetic transition of $LaFe_{11.3}Co_{0.2}Si_{1.5}$ takes place in a narrow temperature range, thus, the corresponding NTE operation-temperature window is relatively narrow. With increasing content of Co, the magnetization gradually increases with decreasing temperature, which gives rise to a gradual and broadened NTE operation-temperature window. As indicated by the slope triangles in Figure 3, the rates of change of the magnetization (dM/dT) with respect to temperature decreases with increasing Co content from 0.2 to 1.0. The results show that the NTE properties are controlled by the dM/dT. (The magnetization of $LaFe_{13-x}Si_x$ (x = 1.5, 1.8, 2.1, and 2.4 can be found in Supporting Information).

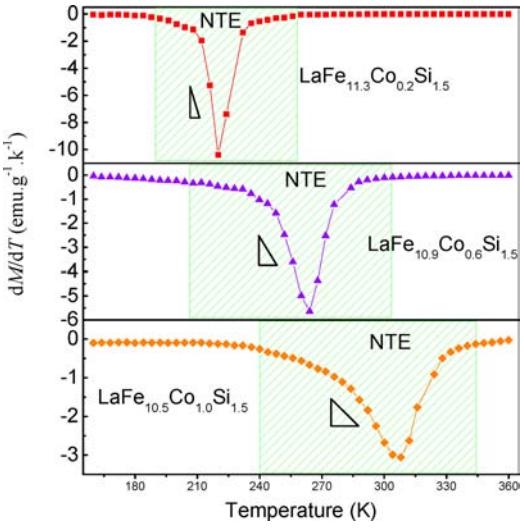

Figure 3. Rate of change of magnetization as a function of temperature for $LaFe_{11.5-x}Co_xSi_{1.5}$ (x = 0.2, 0.6, and 1.0). The slope triangles reflect the changes of dM/dT with respect to temperature in the NTE operation-temperature window.

From a technological viewpoint, La(Fe, $Si)_{13}$-based compound, as a new NTE material, shows a number of advantages over other NTE materials, which is analogous to the doped antiperovskite manganese nitrides.[9] (1) The width and the temperature regions of the NTE operation-temperature window are variable. For example, $LaFe_{10.6}Si_{2.4}$ shows NTE at relatively lower temperatures, whereas the NTE operation-temperature window of the $LaFe_{10.5}Co_{1.0}Si_{1.5}$ covers room temperature. (2) The NTE coefficient is tunable over a wide range of values by adjusting the doping concentration in pure form without forming composites. For example, the $LaFe_{11.3}Co_{0.2}Si_{1.5}$ and the $LaFe_{10.5}Co_{1.0}Si_{1.5}$ show CTEs of $-55.8 \times 10^{-6}\ K^{-1}$ and $-26.1 \times 10^{-6}\ K^{-1}$, respectively. (3) The NTE is isotropic. It maintains the cubic $NaZn_{13}$-type structure in the entire temperature range examined. This property is beneficial in avoiding any transformation-induced microcracking during thermal cycling. (4) This material is mechanically hard and has relatively high thermal conductivity. For many applications, NTE materials that have high thermal conductivity are desirable in order to keep the temperature uniform so as to avoid any thermal stresses. Figure 4 shows the temperature dependence of thermal conductivity for $LaFe_{10.5}Co_{1.0}Si_{1.5}$ in the temperature range of 80–300 K. The value of thermal conductivity is 6 $W\cdot(m\cdot K)^{-1}$ at room temperature, much higher than that of typical oxide NTE materials, among which

dx.doi.org/10.1021/ja405161z | J. Am. Chem. Soc. 2013, 135, 11469–11472

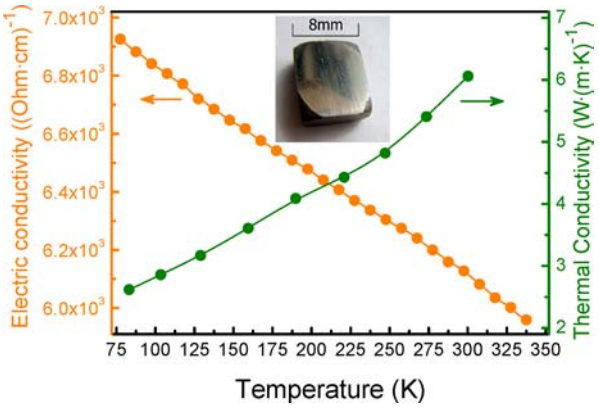

Figure 4. Temperature dependence of thermal conductivity and electrical conductivity for $LaFe_{10.5}Co_{1.0}Si_{1.5}$. (Inset) Photograph of a typical sample of the $LaFe_{10.5}Co_{1.0}Si_{1.5}$.

the thermal conductivity of the ZrW_2O_8 is about 0.51 $W\cdot(m\cdot K)^{-1}$. It is thus suggested that this new NTE material is more advantageous than oxide NTE material as a structural material that requires keeping a homogeneous temperature. (5) This NTE material is of metallic character and therefore electrically conductive. A typical sample of the $LaFe_{10.5}Co_{1.0}Si_{1.5}$ has a metallic luster as shown in the inset of Figure 4. Most of the NTE materials are insulators, which are not applicable in some electrical devices. Thus, there is a need for materials with an NTE coefficient that are also capable of electrical conductivity. Figure 4 also shows the temperature dependence of the electrical conductivity for the $LaFe_{10.5}Co_{1.0}Si_{1.5}$ in the temperature range of 77−340 K. The electrical conductivity of the samples is at a level of about $6-7 \times 10^3$ $(\Omega\cdot cm)^{-1}$. It is clear that the electrical conductivity decreases monotonously with increasing temperature in the entire measured temperature range, being characteristic of metal.

In summary, the sharp change in the volume of in La(Fe, $Si)_{13}$-based compounds was successfully modified into continuous expansion by optimizing the chemical composition. The NTE shifts toward the room temperature region, and the operation-temperature window of NTE becomes broader with increasing the amount of Co dopant in the $LaFe_{11.5-x}Co_xSi_{1.5}$. Typically, a large NTE coefficient of -26.1×10^{-6} K^{-1} in the temperature range from 240 to 350 K and a broad NTE operation-temperature window of 110 K were obtained in the $LaFe_{10.5}Co_{1.0}Si_{1.5}$. Such control of the specific composition and the NTE properties of La(Fe, $Si)_{13}$-based compounds suggests their potential application as NTE materials.

■ ASSOCIATED CONTENT

Ⓢ Supporting Information

The X-ray diffraction patterns at different temperatures. Temperature dependence of magnetization for $LaFe_{13-x}Si_x$ (x = 1.5, 1.8, 2.1, and 2.4). This material is available free of charge via the Internet at http://pubs.acs.org.

■ AUTHOR INFORMATION

Corresponding Author

laifengli@mail.ipc.ac.cn

Notes

The authors declare no competing financial interest.

■ ACKNOWLEDGMENTS

This work was supported by the National Natural Science Foundation of China (Grant No. 51077123), the National Magnetic Confinement Fusion Science Program (Grant No. 2011GB112003), and the fund of the State Key Laboratory of Technologies in Space Cryogenic Propellants, SKLTSCP1204. We thank Prof. WenShan Zhan, Dr. Min Zhou, Dr. Jun Shen, Dr. Zhaoshun Gao, Shanfeng Li, and anonymous reviewers for providing thoughtful comments and suggestions that we used to improve this manuscript, and Shaokui Su for magnetization measurement.

■ REFERENCES

(1) Evans, J. S. O.; Hu, Z.; Jorgensen, J. D.; Argyriou, D. N.; Short, S.; Sleight, A. W. *Science* **1997**, *275*, 61−65.
(2) Hao, Y.; Gao, Y.; Wang, B.; Qu, J.; Li, Y.; Hu, J.; Deng, J. *Appl. Phys. Lett.* **2001**, *78*, 3277−3279.
(3) Takenaka, K. *Sci. Technol. Adv. Mater.* **2012**, *13*, 13001−13011.
(4) Chatterji, T.; Hansen, T. C.; Brunelli, M.; Henry, P. F. *Appl. Phys. Lett.* **2009**, *94*, 241902−3.
(5) Zheng, X. G.; Kubozono, H.; Yamada, H.; Kato, K.; Ishiwata, Y.; Xu, C. N. *Nat. Nanotechnol.* **2008**, *3*, 724−726.
(6) Li, C. W.; Tang, X.; Muñoz, J. A.; Keith, J. B.; Tracy, S. J.; Abernathy, D. L.; Fultz, B. *Phys. Rev. Lett.* **2011**, *107*, 195504.
(7) Greve, B. K.; Martin, K. L.; Lee, P. L.; Chupas, P. J.; Chapman, K. W.; Wilkinson, A. P. *J. Am. Chem. Soc.* **2010**, *132*, 15496−15498.
(8) Chen, J.; Nittala, K.; Forrester, J. S.; Jones, J. L.; Deng, J.; Yu, R.; Xing, X. *J. Am. Chem. Soc.* **2011**, *133*, 11114−11117.
(9) Takenaka, K.; Takagi, H. *Appl. Phys. Lett.* **2005**, *87*, 261902.
(10) Sun, Y.; Wang, C.; Wen, Y.; Zhu, K.; Zhao, J. *Appl. Phys. Lett.* **2007**, *91*, 231913.
(11) Sun, Y.; Wang, C.; Huang, Q.; Guo, Y.; Chu, L.; Arai, M.; Yamaura, K. *Inorg. Chem.* **2012**, *51*, 7232−7236.
(12) Song, X.; Sun, Z.; Huang, Q.; Rettenmayr, M.; Liu, X.; Seyring, M.; Li, G.; Rao, G.; Yin, F. *Adv. Mater.* **2011**, *23*, 4690−4694.
(13) Nakamura, Y.; Takenaka, K.; Kishimoto, A.; Takagi, H. *J. Am. Ceram. Soc.* **2009**, *92*, 2999−3003.
(14) Hu, F.; Shen, B.; Sun, J.; Cheng, Z.; Rao, G.; Zhang, X. *Appl. Phys. Lett.* **2001**, *78*, 3675−3677.
(15) Fujieda, S.; Fujita, A.; Fukamichi, K. *Appl. Phys. Lett.* **2002**, *81*, 1276−1278.
(16) Gschneidner, K. A., Jr.; Pecharsky, V. K.; Tsokol, A. O. *Rep. Prog. Phys.* **2005**, *68*, 1479−1539.
(17) Takenaka, K.; Asano, K.; Misawa, M.; Takagi, H. *Appl. Phys. Lett.* **2008**, *92*, 011927.
(18) Pathak, A. K.; Basnyat, P.; Dubenko, I.; Stadler, S.; Ali, N. *J. Magn. Magn. Mater.* **2010**, *322*, 692−697.
(19) Wang, C. L.; Long, Y. *J. Appl. Phys.* **2013**, *113*, 143902.
(20) Liu, X.; Altounian, Z.; Ryan, D. H. *J. Phys.: Condens. Matter.* **2003**, *15*, 7385−7394.